BJR

Received: 27 March 2012 | Revised: 4 July 2013 | Accepted: 17 July 2013

doi: 10.1259/bjr.20120174

Cite this article as:
Fraioli F, Anzidei M, Serra G, Liberali S, Fiorelli A, Zaccagna F, et al. Whole-tumour CT-perfusion of unresectable lung cancer for the monitoring of anti-angiogenetic chemotherapy effects. Br J Radiol 2013;86:20120174.

FULL PAPER

Whole-tumour CT-perfusion of unresectable lung cancer for the monitoring of anti-angiogenetic chemotherapy effects

[1]F FRAIOLI, MD, [2]M ANZIDEI, MD, [2]G SERRA, MD, [2]S LIBERALI, MD, [2]A FIORELLI, MD, [2]F ZACCAGNA, MD, [3]F LONGO, MD, [4]M ANILE, MD and [2]C CATALANO, MD

[1]Department of Nuclear Medicine, University College London Hospitals, NHS Foundation Trust, London, UK
[2]Department of Radiological Sciences, Sapienza University of Rome, Rome, Italy
[3]Department of Thoracic Surgery, Sapienza University of Rome, Rome, Italy
[4]Department of Medical Oncology, Sapienza University of Rome, Rome, Italy

Address correspondence to: Dr Francesco Fraioli
E-mail: *francesco.fraioli@nhs.net*

Objective: To determine whether CT-perfusion (CT-p) can be used to evaluate the effects of chemotherapy and anti-angiogenic treatment in patients with non-small-cell lung carcinoma (NSCLC) and whether CT-p and standard therapeutic response assessment (RECIST) data obtained before and after therapy correlate.

Methods: 55 patients with unresectable NSCLC underwent CT-p before the beginning of therapy and 50 of them repeated CT-p 90 days after it. Therapeutic protocol included platinum-based doublets plus bevacizumab for non-squamous carcinoma and platinum-based doublets for squamous carcinoma. RECIST measurements and calculations of blood flow (BF), blood volume (BV), time to peak (TTP) and permeability surface (PS) were performed, and baseline and post-treatment measurements were tested for statistically significant differences. Baseline and follow-up perfusion parameters were also compared based on histopathological subclassification (2004 World Health Organization Classification of Tumours) and therapy response assessed by RECIST.

Results: Tumour histology was consistent with large cell carcinoma in 14/50 (28%) cases, adenocarcinoma in 22/50 (44%) cases and squamous cell carcinoma in the remaining 14/50 (28%) cases. BF and PS differences for all tumours between baseline and post-therapy measurements were significant ($p=0.001$); no significant changes were found for BV ($p=0.3$) and TTP ($p=0.1$). The highest increase of BV was demonstrated in adenocarcinoma (5.2±34.1%), whereas the highest increase of TTP was shown in large cell carcinoma (6.9±22.4%), and the highest decrease of PS was shown in squamous cell carcinoma (−21.5±18.5%). A significant difference between the three histological subtypes was demonstrated only for BV ($p<0.007$). On the basis of RECIST criteria, 8 (16%) patients were classified as partial response (PR), 2 (4%) as progressive disease (PD) and the remaining 40 (80%) as stable disease (SD). Among PR, a decrease of both BF (18±9.6%) and BV (12.6±9.2%) were observed; TTP increased in 3 (37.5%) cases, and PS decreased in 6 (75%) cases. SD patients showed an increase of BF, BV, TTP and PS in 6 (15%), 21 (52.5%), 23 (57.5%) and 2 (5%) cases, respectively. PD patients demonstrated an increase of BF (26±0.2%), BV (2.7±0.1%) and TTP (3.1±0.8%) while only PS decreased (23±0.2%).

Conclusion: CT-p can adequately evaluate therapy-induced alterations in NSCLC, and perfusion parameters correlate with therapy response assessment performed with RECIST criteria.

Advances in knowledge: Evaluating perfusional parameters, CT-p can demonstrate therapy-induced changes in patients with different types of lung cancer and identify response to treatment with excellent agreement to RECIST measurements.

In recent years, anti-angiogenic drugs have been rapidly developed and applied as a promising tool for treatment of unresectable lung cancer [1–3], both in combination with first-line conventional chemotherapy or alone as second-line treatment [4,5]. Anti-angiogenic drugs have been demonstrated to inhibit the development of vascular networks in particular by cytostatic rather than cytotoxic effects; therefore, tumour size may not substantially change as a consequence of their action, introducing difficulties for adequate therapy monitoring at imaging follow-up. Functional imaging has been claimed to provide more relevant information on tissue viability during treatment monitoring than the standard therapeutic response assessment (RECIST) based on tumour size changes [6–8], which is currently used. Among other imaging modalities, CT perfusion (CT-p) recently experienced a progressive increase in interest and acceptance in the radiological community for oncological applications [9–13], including both the diagnostic process

and follow-up of lung cancer [14–16]. Substantial differences between treatment response to conventional and anti-angiogenic drugs assessed by RECIST criteria and CT-p in patients with lung adenocarcinoma have been evidenced [17].

Nevertheless, since it has been demonstrated that anti-angiogenic drugs play different roles in the treatment planning of various hystotypes of lung cancer [18], it is plausible that relevant differences may be shown between perfusion CT parameters in lung cancer subgroups, both at baseline and after treatment.

The aim of this study was therefore to determine whether wide-volume CT-p predicts and evaluates anti-angiogenic treatment effects on the whole-tumour mass in patients with different subtypes of locally advanced non-small-cell lung carcinoma (NSCLC) and to determine whether there is a correlation between CT *p*-values and response to therapy according to RECIST criteria.

MATERIALS AND METHODS

Patient population

The study was performed with the approval by the local medical ethics committee, and all the enrolled patients gave their written informed consent to be included in the study group, having been informed about potential benefits and contraindications to CT-p. Between June 2010 and January 2012, 55 patients [38 males, 17 females, age 58±7 (51–82)] with biopsy-proven NSCLC were prospectively enrolled in our study with the following clinical criteria:

(1) Unresectable cancer with maximum size ≥20 mm at a preliminary CT scan (American Joint Committee on Cancer, TNM Stage IIIb or Stage IV).
(2) No previous treatment with chemotherapy or radiation therapy.

Subjects with contraindications to CT-p and/or anti-angiogenic treatment were excluded from the study group. As first-line treatment, all patients received different drug therapies as listed:

– Non squamous carcinoma: carboplatinum area under the curve (AUC) 5 1 q21, paclitaxel 175 mg mq^{-1} 1 q21 or cisplatinum 75 mg mq^{-1} 1 q21, gemcitabine 1250 mg mq^{-1} 1,8 q21, combined with an angiogenesis inhibitor (Bevacizumab) 7,5 mg kg^{-1} 1 q21.
– Squamous cell carcinoma: cisplatinum 75 mg mq^{-1}, docetaxel 75 mg mq^{-1} 1 q21 or cisplatinum 75 mg mq^{-1} 1 q21, vinorelbine 30 mg mq^{-1} 1,8 q21 or cisplatinum 75 mg mq^{-1}, gemcitabine 1250 mg mq^{-1} 1,8 q21.

CT-perfusion technique and image analysis

CT-p imaging was performed with a 64-detector dual-source scanner (Siemens Definition; Siemens Medical Solutions, Forchheim, Germany). Unenhanced breath-hold CT of the lungs (100 kV; 120 mAs; detector configuration, 24×1.2 mm; rotation time, 0.3 s; section thickness, 3.0 mm; reconstruction interval, 3 mm; reconstruction kernel, B30 and B60) was performed to localise the tumour. An expert radiologist (GS, with 2 years of experience in chest CT-p) selected a fixed scanning range for a 136 mm volume in order to include the whole-lesion longitudinal extent. A total of 90 ml of high concentration (350 mg of iodine per ml) non-ionic-iodinated contrast medium (Iomeron® 350; Bracco, Milan, Italy) was injected by using a fractionated administration protocol (30 ml at 4 ml s^{-1}, 10 ml at 2 ml s^{-1} and 50 ml s^{-1} at 1 ml s^{-1}, followed by a 20 mL saline flush at 1 ml s^{-1}). Perfusion imaging started immediately after the injection with a free-breathing dynamic acquisition (100 kV; 120 mAs; detector configuration, 24×1.2 mm; rotation time, 0.3 s; section thickness, 3.0 mm; reconstruction increment, 3 mm; total scanning time, 70 s; four-dimensional range, 136 mm/1.75 s per scan; total scans, 40; reconstruction kernel, B30). All patients were instructed to perform the respiration in a constant manner to avoid excessive lung motion that may hamper postprocessing and prolong image evaluation. All data sets were transferred to a workstation (CT workplace; Siemens Healthcare, Erlangen, Germany) featuring a CT-p software (Syngo Body Perfusion CT, Syngo 2006G; Siemens Medical Solutions) based on a modified PATLAK model [19]. Two radiologists (CC, FF; with 15 and 9 years of experience in interpreting chest CT, respectively) independently reviewed and analysed all examinations in a random order. The unenhanced data sets were available for lesion size assessment (measure of the maximal diameter of the lesion on the axial plane) as prescribed by RECIST criteria. The contrast-enhanced data sets from the dynamic acquisition were then assessed for evaluation of CT-p parameters after applying an automatic three-dimensional motion correction algorithm featuring a previously described non-rigid registration model for reduction of movement artefacts [20]. A circular 1.5 cm^2 region of interest (ROI) was manually placed in the middle of an axial plane of the thoracic aorta, paying attention not to include mural calcifications and to avoid partial volume artefacts, and generating an arterial time-enhancement curve (Figure 1); the whole volume of interest of the tumour was isolated by manual segmentation not including the utmost tumour margins to avoid partial volume effect or inclusion of peritumoural fibrosis. Functional calculations were automatically generated along with colour-coded functional maps of the following parameters: blood flow (BF) in ml per 100 ml per min, blood volume (BV) in ml per 100 ml, time to peak (TTP) in seconds and permeability surface (PS) in ml per 100 ml per min. Response to treatment was evaluated on the basis of RECIST criteria as follows: complete response (CR) if no target lesion was evidenced at follow-up, partial response (PR) if a 30% decrease in the sum of the longest diameter of target lesions was evidenced at follow-up, progressive disease (PD) if a 20% increase in the sum of the longest diameter of target lesions was evidenced at follow-up, and stable disease (SD) if small changes that do not meet above criteria occurred at follow-up.

Figure 1. Image shows the typical arterial curve during perfusional studies; the white curve represents the tumoural enhancement during ΔT.

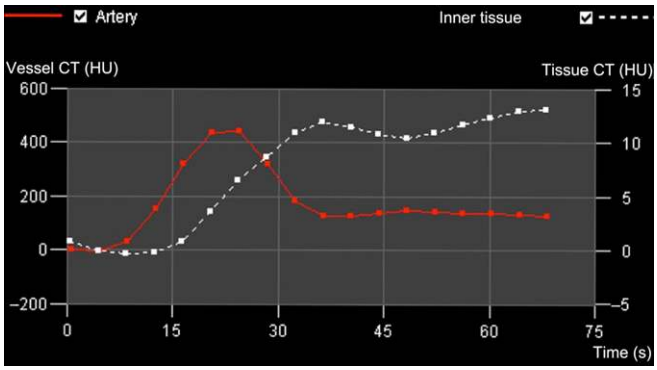

Table 1. Bland–Altman 95% confidence limits of agreement between the two readers for standard therapeutic response assessment (RECIST), CT-perfusion (CT-p) blood flow (BF), CT-p blood volume (BV), CT-p time to peak (TTP) and CT-p permeability (PS) evaluated at baseline and at the end of the follow-up

Measurements or parameters	Baseline		End of follow-up	
	Bias ± standard deviation	95% limits of agreement (from–to)	Bias ± standard deviation	95% limits of agreement (from–to)
RECIST	−3.73±13.94	−31.03 to 23.58	−4.04±14.19	−31.85 to 23.77
CT-p BF	−2.12±2.57	−7.16 to 2.91	−0.36±3.23	−6.69 to 5.96
CT-p BV	−3.66±6.86	−17.12 to 9.79	1.08±7.07	−12.78 to 14.94
CT-p TTP	0.70±7.06	−13.14 to 14.53	−1.43±6.72	−14.61 to 11.75
CT-p PS	−0.45±7.07	−14.31 to 13.41	−1.61±7.20	−15.73 to 12.51

Statistical analysis

The RECIST and CT-p measurements obtained at baseline and 3 months after treatment were transferred to an electronic database (Microsoft Excel 2008 for Macintosh; Microsoft Corporation, Redmond, WA). Statistical analysis was performed using a dedicated software (SPSS® v. 13.0 for Macintosh; SPSS, Chicago, IL). The interobserver agreement for both RECIST and CT-p measurements were analysed by the Bland–Altman method. The RECIST and CT-parameters obtained at the end of follow-up were compared with respective baseline values, and differences were expressed as mean ± standard deviation (minimum–maximum) of decrease/increase. Both RECIST and CT-p parameters analysed at baseline and on the follow-up studies were tested for statistically significant differences using the paired samples *t*-test ($p<0.05$). Baseline and follow-up perfusion parameters of the neoplastic lesions were also compared based on histopathological subclassification (large cell carcinoma, adenocarcinoma and squamous cell carcinoma), and therapy response assessed by RECIST criteria (CR, PR, SD and PD) using the independent samples *t*-test ($p<0.05$).

RESULTS

All patients underwent baseline CT-p of the primary lung cancer within 10±2 (6–12) days before the beginning of therapy, and the second examination was performed within 91±3 (89–94) days. Average room time including patients preparation was 15±2 min. Average dose–length product was 1489 mGy cm±111, and the effective dose was 22.7 mSv±1.3. Three patients were unavailable for follow-up, and two refused the second examination. Thus, 50 patients (30 staged as IIIb and 20 as IV) were definitively included in the longitudinal evaluation. The widest diameter of the tumours measured on the axial plane at the first examination was 5.38±3.7 cm (1.7–16.8). Cancer histological subtypes were: large cell carcinoma in 14/50 (28%) cases, adenocarcinoma in 22/50 (44%) cases and squamous cell carcinoma in the remaining 14/50 (28%) cases.

Interobserver agreement

The interobserver agreement for the evaluation of RECIST parameters assessed by the two readers was very high for both baseline (bias ± standard deviation=−3.73±13.94; 95% limits of agreement=−31.03 to 23.58) and follow-up evaluations (bias ± standard deviation=−4.04±14.19; 95% limits of agreement=−31.85 to 23.77). Also the evaluation of CT-p readings shows high Bland–Altman 95% confidence limits of agreement between the two readers (Table 1).

CT-p measurements before and after therapy

Values of CT-p measurements at baseline and at the end of follow-up are shown in Table 2 and in Figures 2–5. Table 3 shows BF, BV, TTP and PS values per histological classification.

Regarding perfusional parameters, differences for BF and PS values between baseline and post-therapy measurements were significant ($p=0.001$), whereas no significant changes were found for BV ($p=0.3$) and TTP ($p=0.1$).

At baseline, BF was 51±19.6 (18.90–110.46), being 43.5±16.2 (21.7–82.5) at follow-up, with a mean difference of −10.6±25.4 (−41.5 to 67.7). For PS, the baseline value was 16.8±4.2 (11.0–27.4), the follow-up value being 14.4±3.5 (7.9–21.2),

Table 2. Values of standard therapeutic response assessment (RECIST) (mm), CT-perfusion (CT-p) blood flow (BF; mL per 100 ml per min), CT-p blood volume (BV; ml per 100 ml per min), CT-p time to peak (TTP; s) and CT-p permeability (PS; ml per 100 ml per min) evaluated at baseline and at the end of the follow-up. Mean differences are in percentage of increase/decrease between the two measurements [mean ± standard deviation (minimum–maximum)]. *p*-values were calculated using paired samples *t*-test ($p<0.05$)

Measurements or parameters	Baseline	End of follow-up	Mean differences	*p*-value
RECIST	53.82±36.80 (17–168)	43.6±29.6 (170–148)	−17.4±15.8 (−56 to 23)	0.001
CT-p BF	51.0±19.6 (18.90–110.46)	43.5±16.2 (21.7–82.5)	−10.6±25.4 (−41.5 to 67.7)	0.001
CT-p BV	6.5±2.8 (2.6–12.6)	6.2±2.6 (2.6–13.57)	−0.7±27.6 (−39.5 to 74.9)	0.3
CT-p TTP	18.9±4.4 (8.1–27.5)	19.6±5.4 (9.0–28.5)	4.4±19.3 (−17.0 to 64.7)	0.1
CT-p PS	16.8±4.2 (11.0–27.4)	14.4±3.5 (7.9–21.2)	−13.1±13.7 (−51.9 to 14.8)	0.001

Figure 2. The line chart (a) shows the value of blood flow pre and post therapy of the entire population case by case. The box plot (b) summarises the value of blood flow pre and post therapy of the entire population and according to the histological classification. Blood flow values are expressed as ml per 100 ml per min.

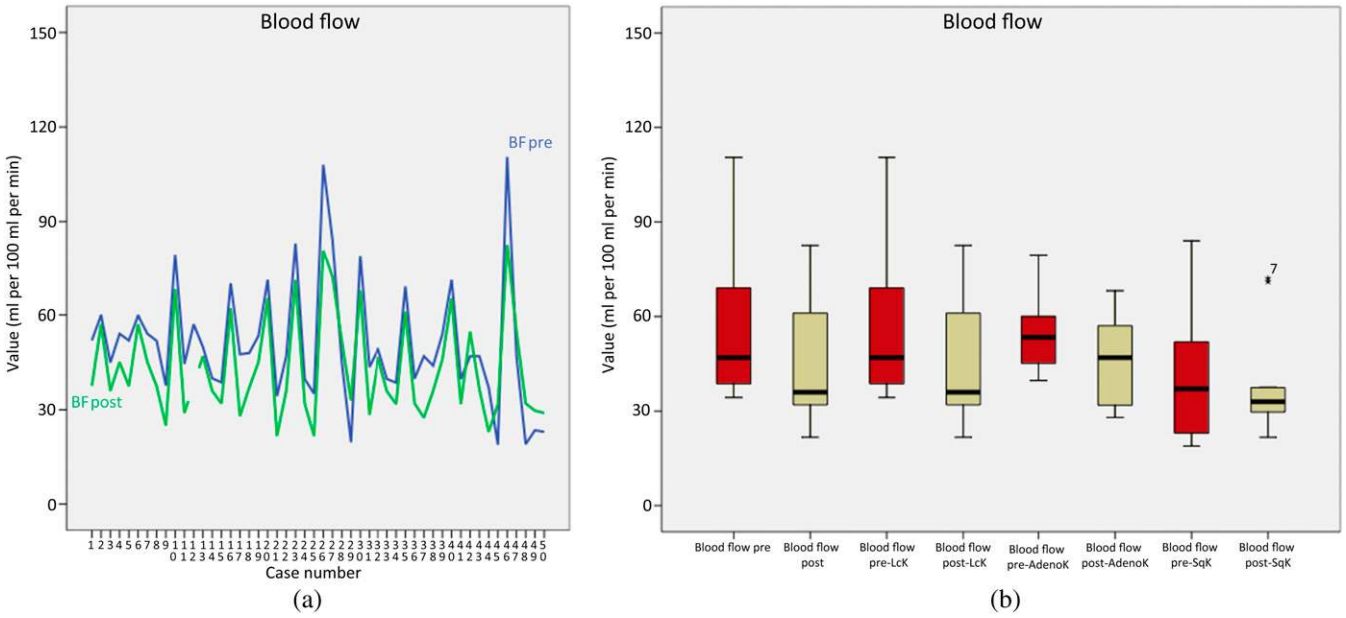

thus determining a mean decrease of −13.1±13.7 (−51.9 to 14.8).

BF had the maximal decrease rate in large cell carcinoma [−19±10% (−36.7 to 0.0)], whereas PS had the highest decrease in squamous cell carcinoma [−21.5±18.5% (4.3–51.9)].

The highest increase of BV was demonstrated in adenocarcinoma [5.2±34.1% (−37.7 to 75.0)], whereas the highest increase of TTP was shown in large cell carcinoma [6.9±22.4% (−13.3 to 56.3)].

In addition to these data, per-histological variations of BF ($0.007<p<0.3$), TTP ($0.15<p<0.8$) and PS ($0.06<p<0.7$) values had so wide ranges that no statistical differences were found at the independent samples *t*-test. A significant difference between the three histological subtypes was demonstrated only for BV ($0.002<p<0.007$).

Figure 3. The line chart (a) shows the value of blood volume pre and post therapy of the entire population case by case. The box plot (b) summarises the value of blood volume pre and post therapy of the entire population and according to the histological classification. Blood volume values are expressed as ml per 100 ml per min.

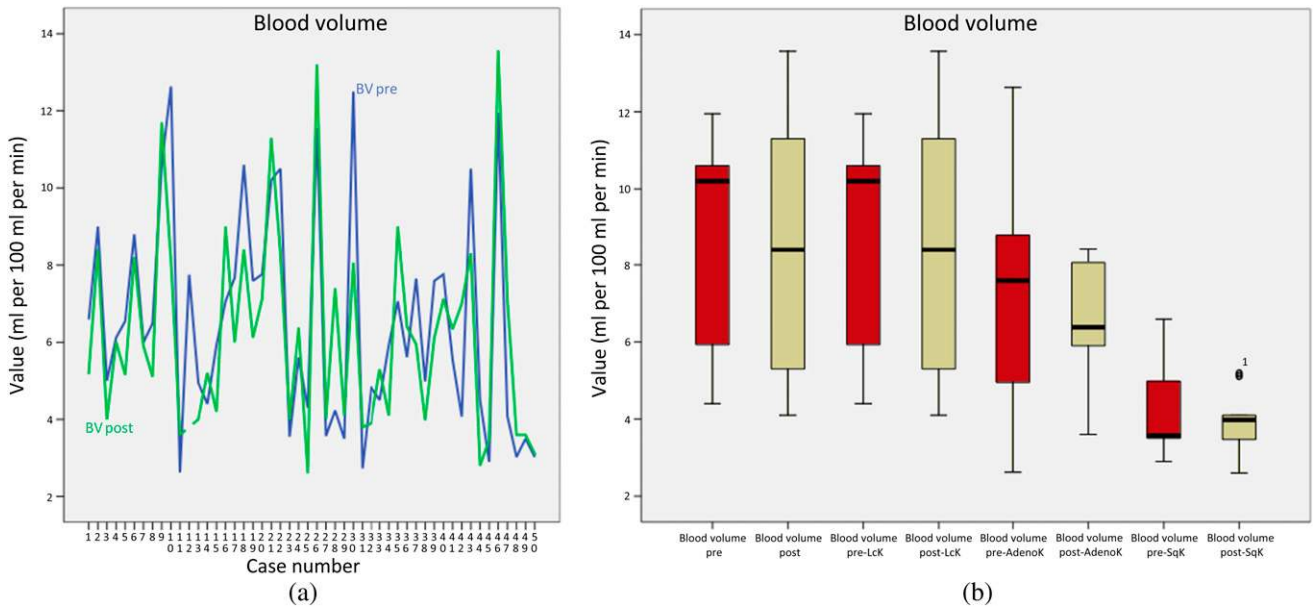

Figure 4. The line chart (a) shows the value of time to peak pre and post therapy of the entire population case by case. The box plot (b) summarises the value of time to peak pre and post therapy of the entire population and according to the histological classification. Time to peak values are expressed in seconds.

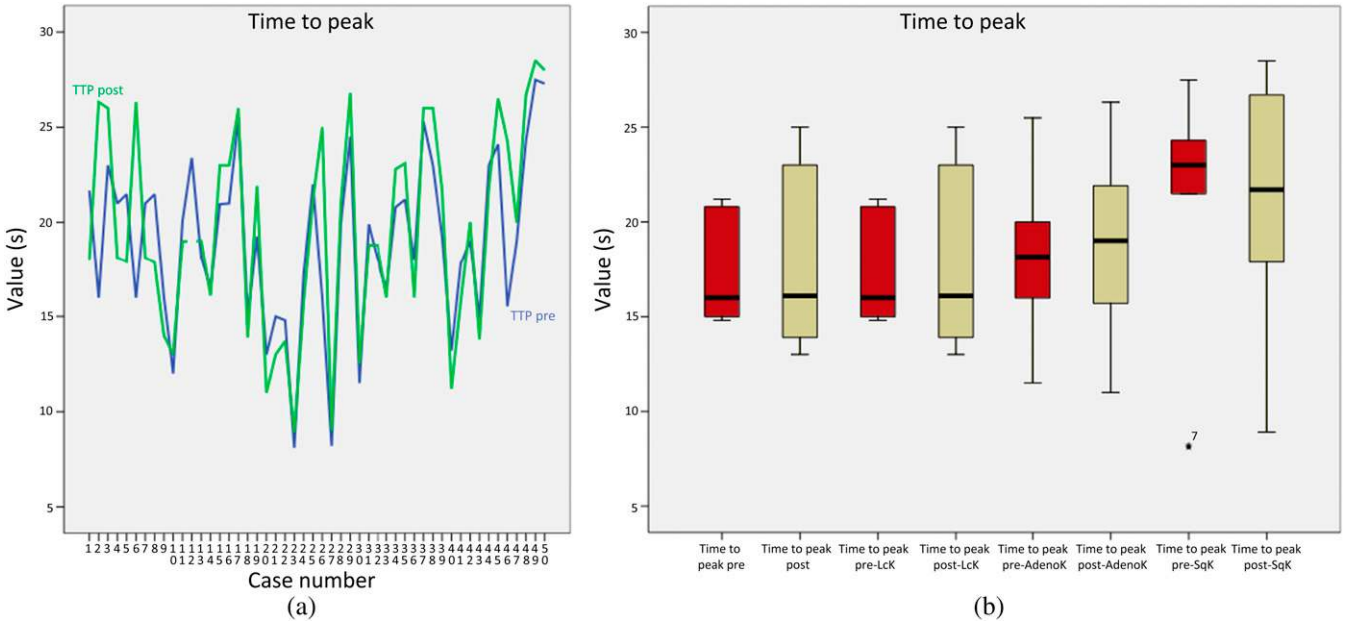

RECIST/CT-p correlation

Values of RECIST and CT-p at baseline and at the end of follow-up are shown in Table 4 and in Figure 6. On the basis of RECIST criteria, 8 (16%) patients were classified as PR, 2 (4%) as PD and the remaining 40 (80%) as SD. No patients showed a complete response to therapy.

PR had a RECIST value of 3.8±2.54 cm (2.2–10) at baseline and a value of 2.4±1.9 cm (1–7) after therapy, showing a decrease percentage of 38.7±10.4% (30–10). All these patients showed a decrease of both BF [18±9.6% (4.6–27.8)] and BV [12.6±9.2% (1.7–21.4)] (Figure 7); TTP increased in 3 (37.5%) cases with a mean increase of 8±36.3% (−16.9 to 64.7); PS decreased in 6 (75%) cases with a mean decrease of 1.1±9.9 (−14.8 to 8.6).

SD had a RECIST value of 5.83±3.8 cm (1.7–16.8) at baseline and a value of 4.8±3 cm (1.5–14.8) after therapy, showing a mean decrease percentage of 15.1±10.7% (12–29%).

Figure 5. The line chart (a) shows value of permeability pre and post therapy of the entire population case by case. The box plot (b) summarises the value of permeability pre and post therapy of the entire population and according to the histological classification. Permeability values are expressed as ml per 100 ml per min.

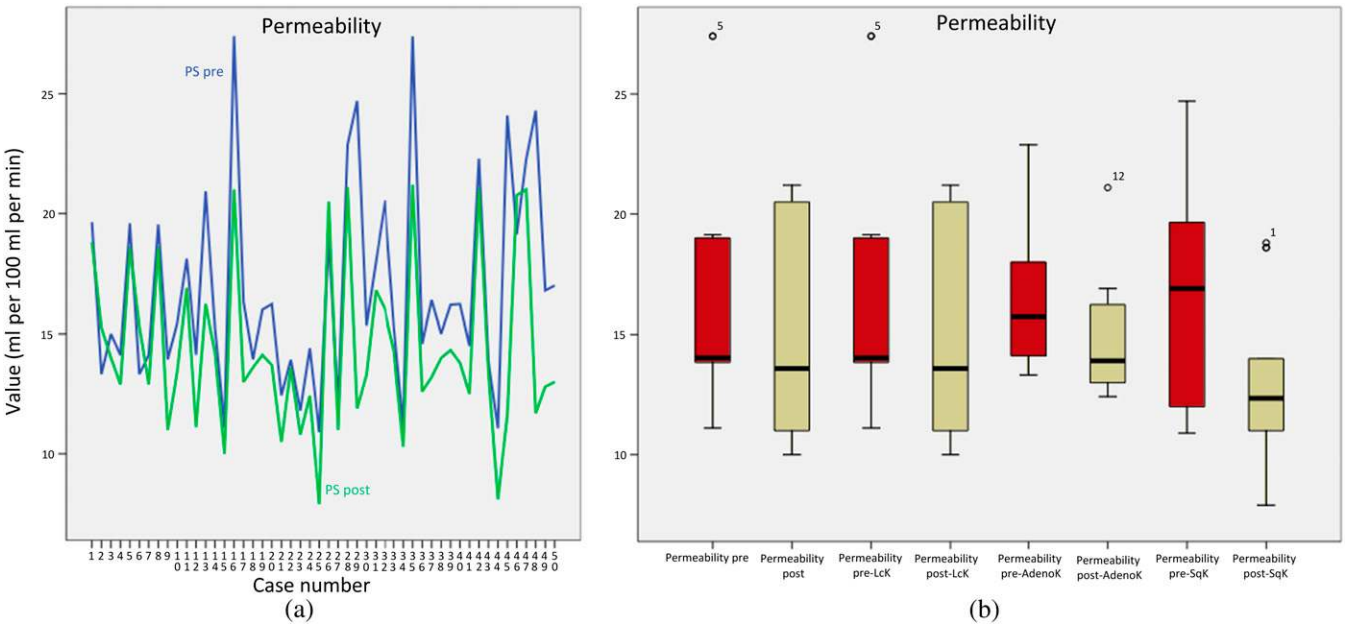

Table 3. Values of CT-perfusion (CT-p) blood flow (BF; ml per 100 ml per min), CT-p blood volume (BV; ml per 100 ml per min), CT-p time to peak (TTP; s) and CT-p permeability (PS; ml per 100 ml per min) evaluated at baseline and at the end of the follow-up considering the histological classification (large cell carcinoma—LcK, adenocarcinoma—AdenoK, squamous cell carcinoma—SqK). All values are expressed as mean ± standard deviation (minimum–maximum) with appropriate units of measurement. *p*-values were calculated using the independent samples *t*-test ($p<0.05$)

Measurements or parameters	Baseline			End of follow-up			Mean differences (%)			*p*-value
	LcK ($n=14$)	AdenoK ($n=22$)	SqK ($n=14$)	LcK ($n=14$)	AdenoK ($n=22$)	SqK ($n=14$)	LcK ($n=14$)	AdenoK ($n=22$)	SqK ($n=14$)	
CT-p BF	56.11±25.00 (34.33–110.50)	53.5±12.0 (39.7–79.4)	42.0±21.6 (18.9–84.0)	44.5±20.2 (21.72–82.49)	46.6±13.8 (27.50–68.12)	37.7±15.2 (21.7–72.0)	−19±10 (−36.7–0.0)	13.3±16.2 (−41.5 to 16.6)	2.0±40.5 (−67 to 38)	$0.007<p<0.300$
CT-p BV	8.46±2.60 (4.4–11.9)	6.6±2.6 (2.62–12.60)	4.4±1.3 (2.9–6.6)	8.6±3.2 (4.1–13.6)	6.3±1.4 (3.6–8.4)	3.9±0.8 (2.6–5.2)	1.2±21.2 (−30.7 to 27.5)	5.2±34.1 (−37.7 to 75.0)	−6.8±21.3 (−19.6 to 39.5)	$0.002<p<0.007$
CT-p TTP	17.7±3 (14.8–23.4)	18.2±3.6 (11.5–25.5)	21.4±5.9 (8.10–27.49)	18.6±4.9 (13–25)	18.9±4.7 (11.0–26.3)	21.6±6.6 (8.9–28.5)	6.9±22.4 (−13.3 to 56.3)	4.6±21.6 (−15.3 to 64.7)	1.5±11.4 (−17 to 13)	$0.15<p<0.80$
CT-p PS	16.3±5.3 (11.1–27.4)	16.9±3.0 (13.3–22.9)	17.2±4.9 (10.9–24.7)	14.7±4.3 (10.0–21.2)	15.0±2.8 (12.42–21.10)	13.0±3.5 (7.9–18.8)	−9.0±10.6 (−8.5 to 23.4)	−10.3±9.5 (−14.9 to 22.4)	−21.5±18.5 (4.3–51.9)	$0.06<p<0.70$

Table 4. Values of standard theropentic response assessment (RECIST) (mm), CT-perfusion (CT-p) blood flow (BF; ml per 100 ml per min), CT-p blood volume (BV; ml per 100 ml per min), CT-p time to peak (TTP; s) and CT-p permeability (PS; ml per 100 ml per min) evaluated at baseline and at the end of the follow-up considering the response to therapy classification (partial response—PR, progressive disease—PD, stable disease—SD). All values are expressed as mean ± standard deviation (minimum–maximum) with appropriate units of measurement

Measurements or parameters	Baseline			End of follow-up			Mean differences (%)		
	PR ($n=8$)	PD ($n=2$)	SD ($n=40$)	PR ($n=8$)	PD ($n=2$)	SD ($n=40$)	PR ($n=8$)	PD ($n=2$)	SD ($n=40$)
RECIST	3.8±2.5 (2.2–10.0)	2.6±0.1 (2.6–2.7)	5.8±3.8 (1.70–1.68)	2.45±1.90 (1–7)	3.15±0.20 (3.0–3.3)	4.8±3.0 (1.5–14.8)	−38.7±10.4 (−30.0 to −56.5)	22.6±0.6 (22.2 to 23.0)	−15.1±10.7 (−29 to 12)
CT-p BF	53.6±4.8 (45–60)	23.20±0.35 (23.0–23.5)	51.9±20.9 (18.9–110.5)	44.10±8.75 (36.0–57.4)	29.3±0.5 (29.0–29.7)	44.1±17.5 (21.7–82.5)	−18.2±9.6 (−27.8 to −4.6)	26.2±0.2 (26.0–26.3)	−10.9±26.7 (−41.5 to 67.7)
CT-p BV	6.8±1.4 (5–9)	3.3±0.3 (3.0–3.5)	6.6±2.9 (2.6–12.6)	5.9±1.5 (4.00–8.41)	3.3±0.35 (3.1–3.6)	6.4±2.7 (2.6–13.6)	−12.6±9.1 (−1.6 to −21.4)	2.7±0.1 (2.6–2.8)	−3.3±30.0 (−39.5 to 75.0)
CT-p TTP	20.2±2.7 (15.9–23.0)	27.40±0.14 (27.3–27.5)	18.2±4.4 (8.1–25.5)	21.00±4.25 (17.85–26.32)	28.20±0.35 (28.0–28.5)	18.9±4.4 (8.9–26.8)	8.0±36.3 (−16.9–64.7)	3.13±0.70 (2.6–3.7)	3.75±15.00 (15.4–56.3)
CT-p PS	16.0±2.9 (13.3–19.6)	16.9±0.1 (16.8–17.0)	16.9±4.5 (10.9–27.4)	15.8±2.5 (12.9–18.8)	12.8±0.2 (12.7–13.0)	14.2±4.5 (10.9–27.4)	−1±9.9 (−8.64 to 14.80)	−23.6±0.2 (−23.8 to −23.5)	−14.9±13.8 (−51.8 to 8.5)

Figure 6. The line chart (a) shows the value of standard therapeutic response (RECIST) pre and post therapy of the entire population case by case. The box plot (b) summarises the value of RECIST pre and post therapy of the entire population and according to the histological classification. RECIST values are expressed in millimetres.

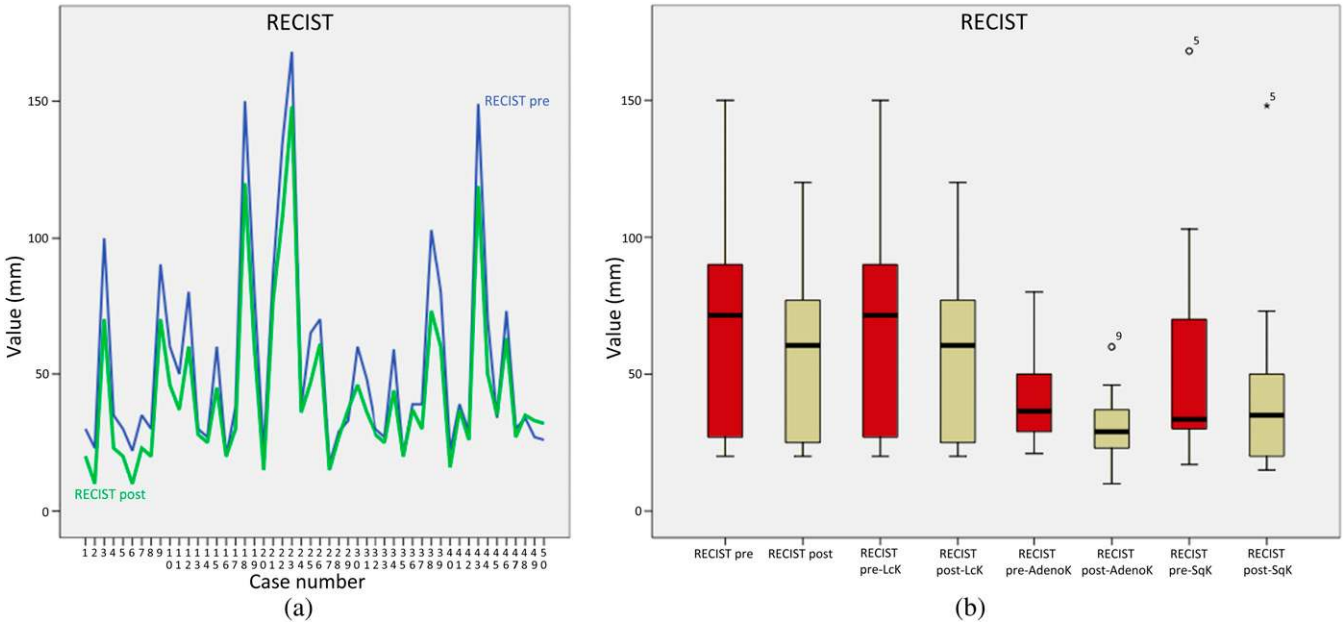

Among these cases, only 6 (15%) showed an increase of BF, whereas the mean rate of decrease was 10.9±27.7% (−41.4 to 67.7) (Figure 8). BV has grown in 21 (52.5%) cases with a mean increase rate of 3.2±30% (−39.5 to 75). TTP has grown in 23 (57.5%) cases with a mean increase rate of 3.7±15% (−15.4 to 56). PS values showed an increase in only 2

Figure 7. A 67-year-old male with a diagnosis of Stage IV squamous cell carcinoma of the left lower lobe. At baseline examination, sagittal reformation shows a 28 mm lesion; CT-perfusion (CT-p) parameters were, respectively: blood-flow (BF)=42.7 ml per 100 ml per s (a), blood volume (BV)=4.2 ml per 100 ml per min (b), time to peak (TTP)=27.2 s (c), permeability (PS)=23.4 ml per 100 ml per min (d). At the follow-up examination, the maximum diameter of the lesion was 30 mm; CT-parameters were, respectively: BF=37.6 ml per 100 ml per s (e), BV=3.7 ml per 100 ml (f), TTP=23.6 s (g), PS=20.6 ml per 100 ml per min (h). The lesion was considered stable on the basis of standard therapeutic response (RECIST) measurements while the changes observed at CT-p were considered to be consistent with therapy-induced response of cancer tissue.

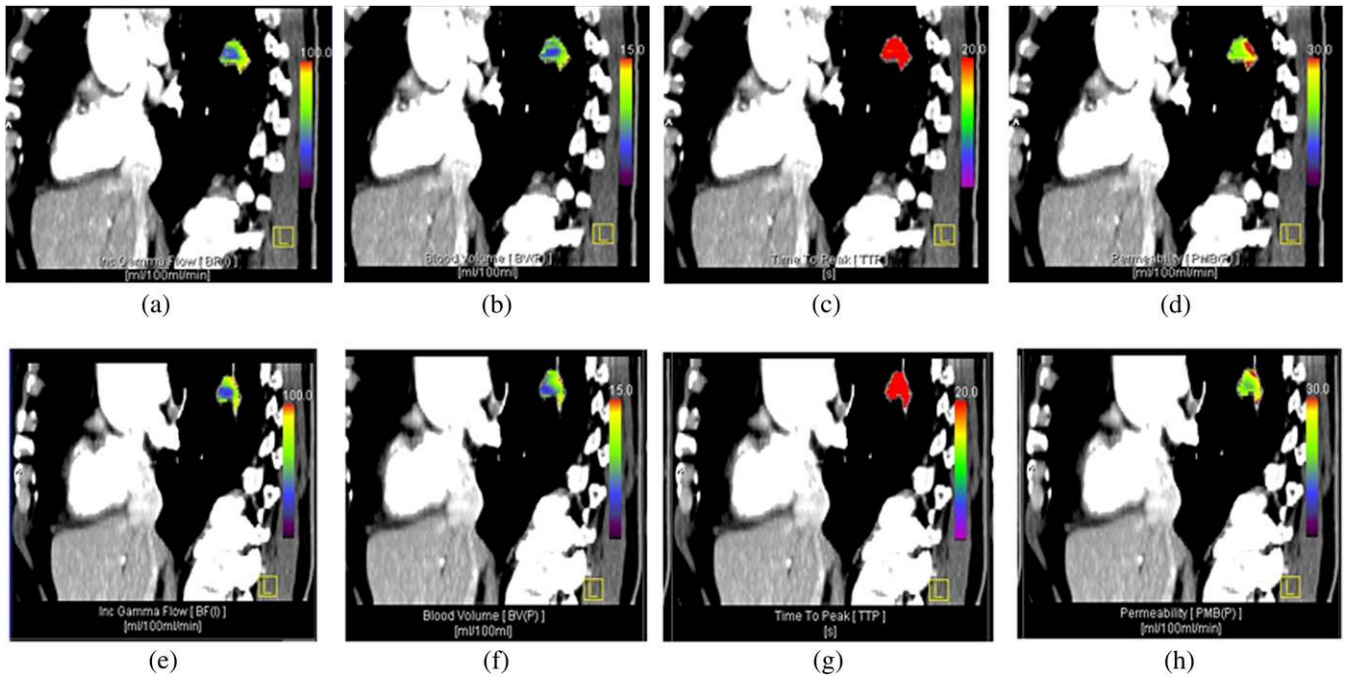

Figure 8. A 69-year-old male with a diagnosis of Stage IIIb adenocarcinoma of the right upper lobe. Baseline axial (a) and multiplanar reconstructed images in the coronal (b) and sagittal (c) planes show the colour-coded mapping of the blood flow (BF) values over the whole-tumour volume. Axial (d), coronal (e) and sagittal (f) views obtained after therapy demonstrate both a decrease of lesion size [standard therapeutic response assessment (RECIST) partial response] and a global reduction of BF.

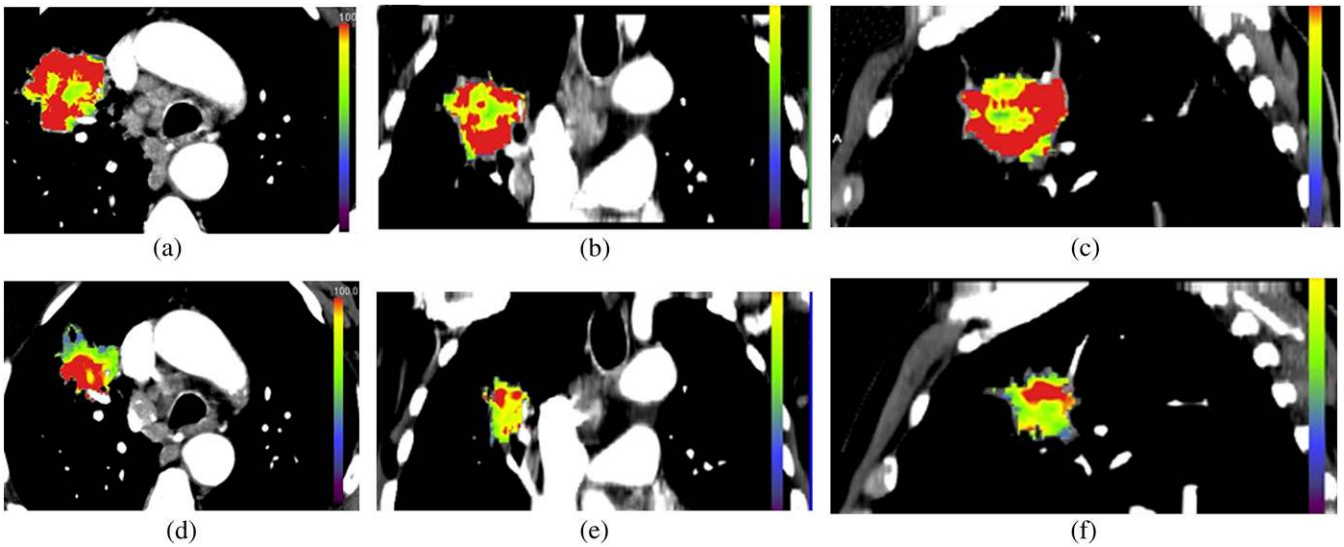

(5%) cases, so the mean decrease rate was 14.9±13.4% (−51.9 to 8.5).

PD patients had a RECIST value of 2.65±0.1 cm (2.6–2.7) at baseline and a value of 3.15±0.2 cm (3.0–3.3) after therapy, showing an increase percentage of 22.6±0.6% (23–22.2).

In these patients, we demonstrated an increase of BF [26±0.2% (26–26.5)], BV [2.7±0.1% (2.6–28)] and TTP [3.1±0.8% (2.6–3.7)] while only PS decreased [23±0.2% (23.5–23.8)].

Comparing baseline values of BF, BV, TTP and PS, no significant differences were noted between PD and SD for all CT-p values ($p<0.8$); the same finding was observed between SD and PR for BF, BV and PS ($p<0.9$) and between PR and PD for PS ($p=0.7$). Significant differences were shown between SD and PD for TTP ($p=0.06$) and between PR and PD for BF ($p=0.001$), BV ($p=0.008$) and TTP ($p=0.007$) (Figure 9).

DISCUSSION

In our study, we investigated if CT-p may allow evaluation of the effects of combined chemotherapy on different subtypes of NSCLCs

Figure 9. A 66-year-old male with a diagnosis of Stage IV adenocarcinoma of the left upper lobe. Axial images show colour-coded maps of blood flow (BF), blood volume (BV), time to peak (TTP) and permeability (PS) before (a–d) and after (e–h) therapy. At follow-up, standard therapeutic response assessment (RECIST) measurements demonstrated a 30% decrease in size (partial response), whereas CT-perfusion (CT-p) evaluation showed a 20% decrease of BF, a 5% increase of BV, a 4% increase of TTP and a 14% decrease of PS.

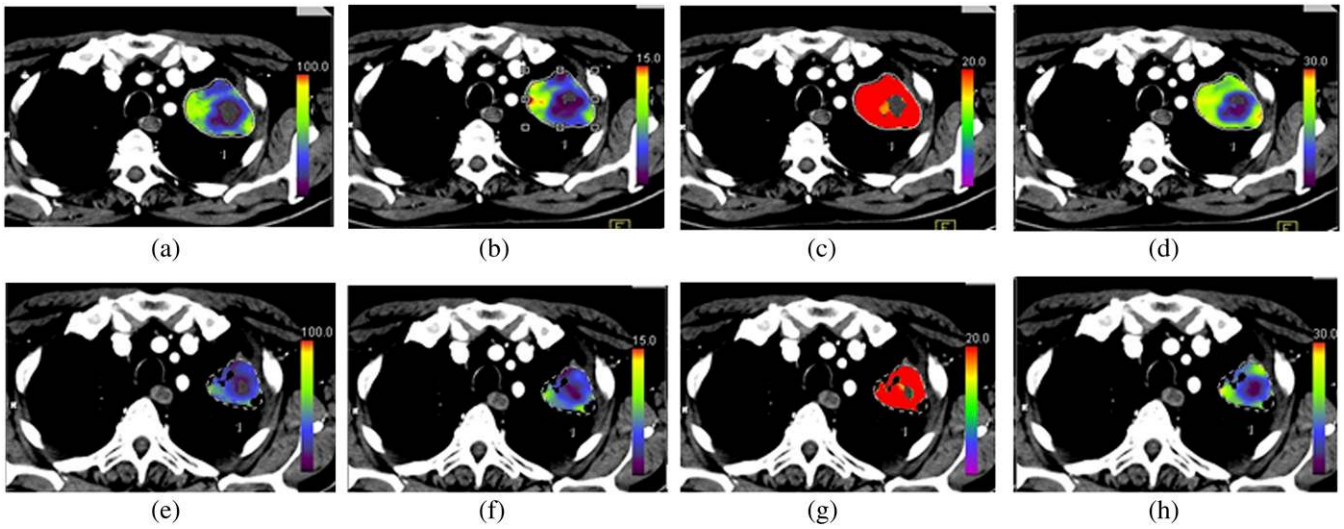

and if changes in CT-p values correlate with response to therapy as presently assessed by conventional RECIST criteria. Although an exhaustive prediction of treatment outcome is at present out of range, our results showed that some therapy-induced changes could be anticipated on the basis of CT-p parameters of the lesions at baseline examinations. In particular, baseline values of BF, BV and TTP were different among PR, PD and SD patients. However, these differences were significant for TTP only between SD and PD patients ($p=0.06$), and between PR and PD patients for BF ($p=0.001$), BV ($p=0.008$) and TTP ($p=0.007$).

In particular, the 8 subjects classified as RECIST-PR showed a significant decrease in BF and BV after therapy, whereas PS decreased in 6 (75%) and increased in 2 (25%), and finally TTP decreased in 5 (62.5%) and increased in 3 (37.5%). In RECIST-SD subjects, no significant variations of the CT-p parameters were evidenced after therapy, whereas in the 2 patients classified as RECIST-PD, BF, BV and TTP were increased at follow-up and PS was decreased.

The highest values of BF and BV at baseline have been demonstrated for large cell carcinoma, whereas the highest values of TTP and PS have been shown for squamous cell carcinoma. These results could be of some interest in order to address a prognostic value to the CT-p data for the different hystotypes and RECIST classes. With regard to the variation of CT-p parameters, depending on lesions subtypes, the higher BF decrease after therapy was demonstrated in large cell carcinoma. For both BV and PS, the highest decrease rates were shown in squamous cell carcinoma. TTP values increased in all the three types of carcinoma, but the highest increase was recorded in large cell carcinoma and the lowest values in squamous cell carcinoma. These findings were somewhat unexplored in previous studies and may be of some importance for treatment strategies. However, we have to admit that lesion localisation and size and patients' ages may play a relevant role in determining the physiopathology of lung cancer and influencing CT-p measurements, but these parameters were not significantly taken into account in our study.

The discrepancies between RECIST and CT-p measurements are probably even more significant from a clinical point of view: in five subjects, the size of the lesion was stable at follow-up or showed a negligible increase while vascularisation was increased, suggesting a poor response to treatment. Indeed, these findings emphasise the hypothesis that the differences between RECIST criteria and CT-p parameters may be relevant to assess physiological response to therapy even in an early phase, monitoring and detecting subtle differences in biological activities. It is therefore plausible that a CT-p evaluation performed even after a short-time interval from the beginning of therapy may be helpful for clinical planning and may correlate with a better prognosis if therapy is changed on time.

In addition to this, it is worthwhile to underline that understanding the CT-p technique requires knowledge of a few specific technical concepts. Firstly, a small-fractionated contrast medium administration is necessary to fit the theoretical basis of the Patlak algorithm used to analyse perfusion CT data. Secondly, the rotating movement of the scanner allows a real-time volumetric perfusional evaluation rather than that reported on a single arbitrary section or a small proportion of the lesions, as still reported in recent studies performed with 64-or even 16-section multidetector CT [21]. Finally, radiation exposure with respect to the scan parameters is a risk; although radiation exposure for CT-p is small compared with the RT doses that many patients with lung cancer are likely to receive, it is important to establish protocols with the minimum dose possible for quality measurements. In this regard, we adopted a combined strategy in order to keep the radiation dose as low as possible without compromising the overall image quality: using an intermediate tube voltage (100 kV) and a low tube current (120 mAs), the effective radiation dose was 22.7 ± 1.3 mSv. Other possible solutions to further reduce the radiation exposure are the doubling of the interscan delay and the reduction of the scan length to the minimum with smaller lesions.

We recognise that our study has some relevant limitations. The major drawback is represented by the fact that no histological validation study has been performed to evaluate the congruence between CT-p variations and treatment-induced changes in cancer tissue, hence no reduction in vascularisation was detected. However, pathological proof for chest lesions may be invasive and technically difficult, whereas it is possible and reasonable in other sites such as the rectum or liver. There is no gold standard for the evaluation of response to therapy while monitoring such a combined chemotherapy; in this study, we chose simply to integrate perfusional data with the current method to evaluate therapy response, the RECIST criteria.

Moreover, the follow-up was limited to a single examination performed within 3 months from the beginning of therapy, which was obviously heterogeneous in the three histological subtypes; as a consequence of this, long-term prognostic evaluation of perfusion parameters was not possible.

However, it must be underlined that percentage changes in perfusional parameters at follow-up are statistically not very different from the baseline and thus may lie within the normal range of variability. Regarding this point, a further limitation of this study is that no reproducibility analysis in this cohort has been produced.

Finally, other authors adopted different acquisition protocols, including other contrast-medium technical issues [22]. This point is still debated depending on the equipment and particularly the reconstruction algorithm used.

In conclusion, our results suggest that differences in CT-p parameters between subtypes of lung cancer before and after therapy may play an important role in determining the physiopathology of lung cancer and may be relevant to assess response to therapy even at an early stage. Managing to monitor even subtle differences in biological activities, CT-p may be helpful for therapeutical planning and may lead to better prognostic results if therapies are changed when needed.

REFERENCES

1. Folkman J. What is the evidence that tumors are angiogenesis dependent? J Natl Cancer Inst 1990;82:4–6.
2. Fontanini G, Vignati S, Boldrini L, Chinè S, Silvestri V, Lucchi M, et al. Vascular endothelial growth factor is associated with neovascularization and influences progression of non-small cell lung carcinoma. Clin Cancer Res 1997;3: 861–5.
3. Mattern J, Koomagi R, Volm M. Vascular endothelial growth factor expression and angiogenesis in non-small cell lung carcinomas. Int J Oncol 1995;6:1059–62.
4. Sandler A, Gray R, Perry MC, Brahmer J, Schiller JH, Dowlati A, et al. Paclitaxel–carboplatin alone or with bevacizumab for non-small-cell lung cancer. N Engl J Med 2006;355: 2542–50. doi: 10.1056/NEJMoa061884
5. Shepherd FA, Rodrigues Pereira J, Ciuleanu T, Tan EH, Hirsh V, Thongprasert S, et al. Erlotinib in previously treated non-small-cell lung cancer. N Engl J Med 2005;353:123–32. doi: 10.1056/NEJMoa050753
6. World Health Organization. WHO handbook for reporting results of cancer treatment. Offset Publication No.48. pp. 1–42. Geneva, Switzerland: World Health Organization; 1979. Available from http://whqlibdoc.who.int/offset/WHO_OFFSET_48.pdf
7. Therasse P, Arbuck SG, Eisenhaueer EA, Wanders J, Kaplan RS, Rubinstein L, et al. New guidelines to evaluate the response to treatment in solid tumors: European Organization for Research and Treatment of Cancer, National Cancer Institute of Canada. J Natl Cancer Inst 2000;92:205–16.
8. Kerbel R, Folkman J. Clinical translation of angiogenesis inhibitors. Nat Rev Cancer 2002; 2:727–39. doi: 10.1038/nrc905
9. Stevenson JP, Rosen M, Sun W, Gallagher M, Haller DG, Vaughn D, et al. Phase I trial of the antivascular agent combretastatin A4 phosphate on a 5-day schedule to patients with cancer: magnetic resonance imaging evidence for altered tumor blood flow. J Clin Oncol 2003;21:4428–38. doi: 10.1200/JCO.2003.12.986
10. Yi CA, Lee KS, Kim EA, Han J, Kim H, Kwon OJ, et al. Solitary pulmonary nodules: dynamic enhanced multidetector row CT study and comparison with vascular endothelial growth factor and microvessel density. Radiology 2004;233:191–9. doi: 10.1148/radiol.2331031535
11. Ma SH, Le HB, Jia BH, Wang ZX, Xiao ZW, Cheng XL, et al. Peripheral pulmonary nodules: relationship between multi-slice spiral CT perfusion imaging and tumor angiogenesis and VEGF expression. BMC Cancer 200830;8:186. doi: 10.1186/1471-2407-8-186
12. Feng ST, Sun CH, Li ZP, Mak HK, Peng ZP, Guo HY, et al. Evaluation of angiogenesis in colorectal carcinoma with multidetector-row CT multislice perfusion imaging. Eur J Radiol 2010;75:191–6. doi: 10.1016/j.ejrad.2009.04.058
13. Goh V, Halligan S, Daley F, Wellsted DM, Guenther T, Bartram CI. Colorectal tumor vascularity: quantitative assessment with multidetector CT—do tumor perfusion measurements reflect angiogenesis? Radiology 2008;249:510–17. doi: 10.1148/radiol.2492071365
14. Ng QS, Goh V, Klotz E, Fichte H, Saunders MI, Hoskin PJ, et al. Quantitative assessment of lung cancer perfusion using MDCT: does measurement reproducibility improve with greater tumor volume coverage? AJR Am J Roentgenol 2006;187:1079–84. doi: 10.2214/AJR.05.0889
15. Ng QS, Goh V, Fichte H, Klotz E, Fernie P, Saunders MI, et al. Lung cancer perfusion at multi-detector row CT: reproducibility of whole tumor quantitative measurements. Radiology 2006;239:547–53. doi: 10.1148/radiol.2392050568
16. Park MS, Klotz E, Kim MJ, Song SY, Park SW, Cha SW, et al. Perfusion CT: noninvasive surrogate marker for stratification of pancreatic cancer response to concurrent chemo- and radiation therapy. Radiology 2009;250:110–17. doi: 10.1148/radiol.2493080226
17. Fraioli F, Anzidei M, Zaccagna F, Mennini ML, Serra G, Gori B, et al. Whole-tumor perfusion CT in patients with advanced lung adenocarcinoma treated with conventional and antiangiogenetic chemotherapy: initial experience. Radiology 2011;259:574–82. doi: 10.1148/radiol.11100600
18. Rosell R, Carcereny E, Gervais R, Vergnenegre A, Massuti B, Felip E, et al. Erlotinib versus standard chemotherapy as first-line treatment for European patients with advanced EGFR mutation-positive non-small-cell lung cancer (EURTAC): a multicentre, open-label, randomised phase 3 trial. Lancet Oncol 2012;13:239–46. doi: 10.1016/S1470-2045(11)70393-X
19. Patlak CS, Blasberg RG, Fenstermacher JD. Graphical evalutaion of blood-to-brain transfer constants from multiple-time uptake data. J Cereb Blood Flow Metab 1983;3:1–7.
20. Saddi KA, Chefd'hotel C, Cheriet F. Large deformation registration of contrast-enhanced images with volume-preserving constraint. In: Pluim JPW, Reinhardt JM, editors. Proceedings of SPIE: Medical Imaging 2007 Image Processing, Vol 6512. Bellingham, WA: Spie-the International Society for Optical Engineering; 2007. p. 651203.
21. Li Y, Yang ZG, Chen TW, Deng YP, Yu JQ, Li ZL. Whole tumour perfusion of peripheral lung carcinoma: evaluation with first-pass CT perfusion imaging at 64-detector row CT. Clin Radiol 2008;63:629–35. doi: 10.1016/j.crad.2007.12.012
22. Miles KA, Lee TY, Goh V, Klotz E, Cuenod C, Bisdas S, et al. Current status and guidelines for the assessment of tumour vascular support with dynamic contrast-enhanced computed tomography. Eur Radiol 2012;22: 1430–41. Epub 2012 Feb 26. doi: 10.1007/s00330-012-2379-4